Application of Narrow Band Control to Reduce Vibrations in Magnetic Bearing Systems

Monique S. Gaffney
Bruce G. Johnson
SatCon Technology Corporation
12 Emily Street
Cambridge, MA 02139

The goal of this paper is to illustrate the benefits of narrowband control theory for simple, open-loop stable systems, then discuss how the control approach changes for magnetic bearing systems, which are open-loop unstable. Magnetic bearing systems are good applications for narrowband control theory. This paper discusses two sources of synchronous forces, the measurement error and the magnetic unbalance. Both the measurement error and the magnetic unbalance manifest themselves as synchronous disturbances (ref. 1). As will be shown, narrowband control theory for simple, open-loop stable systems provides excellent performance and good stability robustness. Because magnetic bearing systems are open-loop unstable, the narrowband control approach becomes more complex. Disturbance accommodating control (DAC) theory is introduced herein as an effective approach to reduce vibrations in magnetic bearing systems. It is used to develop a control/estimation scheme that enables the rotor to spin about its center of mass, in the presence of the measurement error disturbances.

OVERVIEW

- Magnetic bearing systems are narrowband control applications
- Narrowband control theory for open-loop stable plants
- Narrowband control theory for magnetic bearing systems
- Satcon magnetic bearing system background
- Results from a disturbance accommodating controller

Active control enables magnetic bearings to reduce vibrations in rotating machinery. One method of reducing the synchronous vibrations of a rotating system is to enable the rotor to spin about its true inertial axis. No synchronous forces are generated when the rotor spins about its center of mass because the acceleration of the center of mass of the rotor is zero. The figure below is a simplified free body diagram showing the forces acting between the rotor and stator in a magnetic bearing system. The figure presents an axial cross-section of the gap in a magnetic bearing system. For simplicity, the effects of gravity are neglected; nevertheless with gravity the conclusions are the same. Similarly, the angular motion is neglected, therefore the distance between the forces on the free body diagram is immaterial. The translational equation of motion for the rotor in one radial direction is,

$$m\ddot{x} = F_b + F_d$$

The system will produce no net force on the rotor when,

$$F_b + F_d = 0$$

From the first equation, the acceleration of the center of mass of the rotor, $\ddot{x}$, must be zero for the second equation to be true. If the rotor spins at a constant speed about an axis other than its inertial axis, the center of mass is accelerated due to the changing direction of its velocity vector. This implies that when the axis of rotation is the inertial axis, such that $x = 0$, then there is no net force generated by the bearing system because the acceleration of the center of mass is zero, namely $\ddot{x} = 0$. In summary, spinning the rotor about its inertial axis eliminates the vibratory forces generated by the bearing system. However, the bearing control force F_b is not necessarily zero because it acts to "cancel" any other force Fd_d.

SPIN ABOUT THE CENTER OF MASS

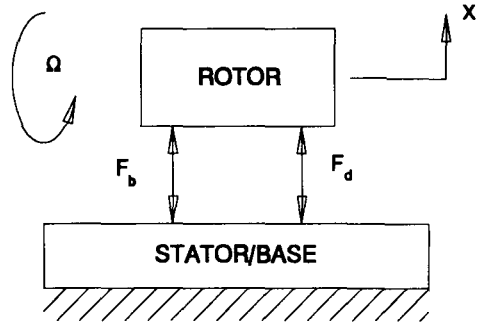

Rotor/Stator Force Interaction

F_b is the bearing force
F_d is any force acting directly between the rotor and base
ie. magnetic unbalance force

Equations of Motion

$m\ddot{x} = F_b + F_d$
want $F_b + F_d = 0$

Bearing force "cancels" disturbance force for no vibrations

The figure below consists of a radial cross-section of a magnetic bearing system. The center of mass (M) is situated on the inertial axis of the rotor. Although its position is unknown, the inertial axis is the desired axis of rotation in order to minimize system vibrations as discussed previously. The measurement center (S) is defined by the position measurement sensors. The position sensors are mounted on the bearing housing and measure the distance to the rotor surface, or in other words, the gap. To give a physical perception of this center, the measurement center is the geometric center of the rotor, assuming an ideal surface measurement, (ie. the rotor surface is perfectly smooth and the material is perfectly homogenous). The line segment (ϵ_S) in the figure below is the unknown distance between the position the sensors measure and the position of the center of mass of the rotor. In conventional bearing systems, this distance is the mass imbalance. Consequently, (ϵ_s) is termed the measurement error because it is the amount of synchronous corruption of the center of mass position signal by the measurement system. Also from the figure, the kinematic relationship relating the center of mass to the measurement center, using complex coordinates, is

$$z_S = z + \epsilon_S e^{j\Omega t}$$

The effect of the measurement error or "mass imbalance" is to produce an additive disturbance at the output of the plant. The output disturbance is also a function of the synchronous frequency.

MEASUREMENT ERROR MODELLING

Goal - vibration reduction ==> spin about the center of mass

Problem - cannot measure the center of mass

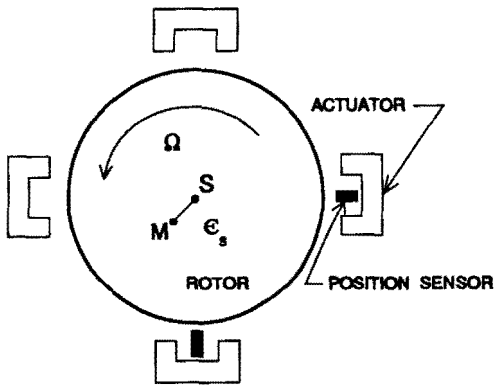

M - rotor center of mass

S - rotor measurement center ~ rotor geometric center

Kinematic relationship (complex notation) $Z_S = Z + \varepsilon_S e^{j\Omega t}$

Additive output disturbance

The following figure is a simple block diagram of a magnetic bearing system, illustrating how the measurement error is an additive plant output disturbance that corrupts the center of mass position. Because the feedback signal, the measured position, is a combination of the inertial position and the measurement error disturbance, the controller drives the rotor to spin about its measurement center. As a result, the rotating system generates vibratory forces.

BLOCK DIAGRAM WITH MEASUREMENT ERROR

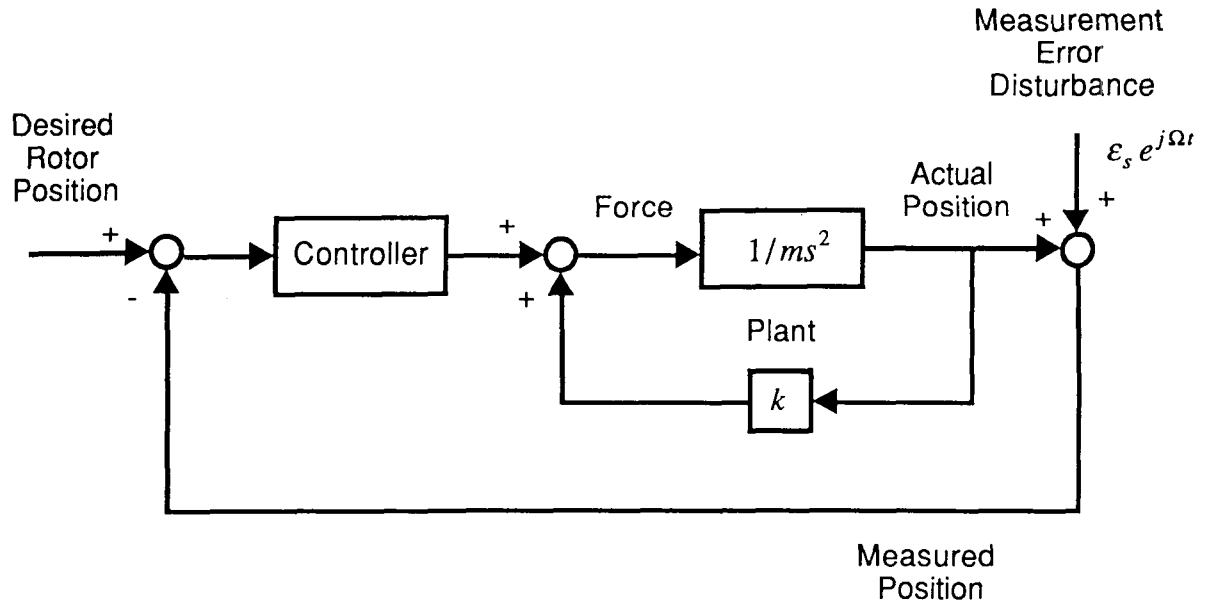

Another synchronous disturbance source is the magnetic unbalance. A magnetic center (F) is located axially along the rotor at each rotor/stator set, for example at the bearings and motor. All the rotor/stator sets on the shaft contribute to a resultant magnetic center. This center is the point of equilibrium for the resultant unstable spring force. In other words, if the rotor spins about its magnetic center, the change in magnetic gap (δG) would be zero. This center depends mainly upon the geometry of the rotor. Given a system with the
bearings as the only source of side-loading forces, the magnetic center is the measurement center (or geometric center), assuming an ideal rotor surface measurement, with a smooth rotor surface and homogenous material properties. Consequently, the position of the magnetic center at each bearing is known from the position sensors. However, if the rotor has other electric components on it, such as an induction motor, the position of the magnetic center at these components cannot be extracted simply from information via sensors at the bearings. Therefore, the resultant magnetic center is unknown and is different than the measurement center. The point (F) in the figure below represents the magnetic center of the rotor at one rotor/stator set. As the rotor spins about its center of mass (M), the distance (ϵ_F) rotates with angular velocity (Ω). The kinematic relationship between the center of mass and the magnetic center, in complex coordinates, is given by

$$z_F = z + \epsilon_F e^{j\Omega t}$$

MAGNETIC UNBALANCE MODELLING

Electric machine interaction ==> radial attractive force ==> function of gap

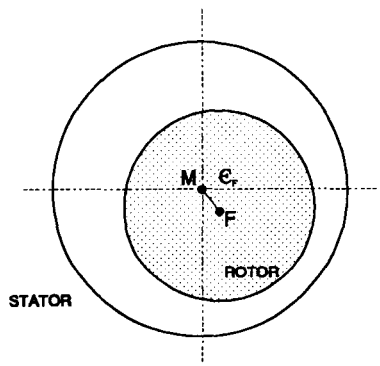

M - rotor center of mass
F - magnetic (field) center ≈ rotor geometric center

Linearized constitutive relation

$F = K \Delta Z_G$ **K < 0, negative stiffness**
$F = K Z_F$ **assuming no base motion**

Kinematic relationship (complex notation)

$z_F = z + \varepsilon_F e^{j\Omega t}$
$F = K z_F = K z + K\varepsilon_F e^{j\Omega t}$ **==> additive input disturbance**

The linearized constitutive relation for the side-loading forces from either the bearings or the motor is

$$F = - K \delta z_g$$

Assuming the rotor/stator set in question is located axially at the center of mass initially to avoid the angular terms, and also assuming no baseplate motion,

$$F = K z_F$$

because the change in magnetic gap is represented by a change in position of the magnetic center, where $(\delta z_F) = -(\delta z_g)$. Thus, combining this equation with the kinematic relation, the expression for the unstable spring force becomes

$$F = K z + K \epsilon_F e^{j\Omega t}$$

As shown in the block diagram below, the synchronous magnetic unbalance disturbances manifests itself as an additive input disturbance.

BLOCK DIAGRAM WITH BOTH DISTURBANCE INPUTS

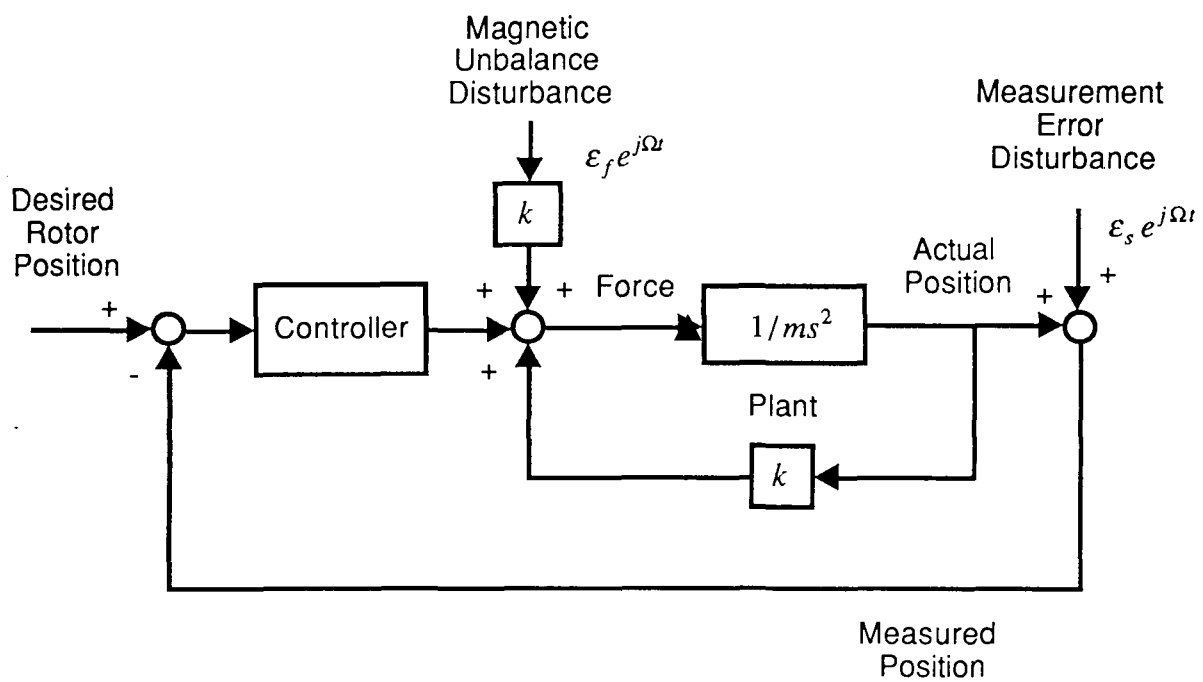

Narrowband control theory for open-loop stable plants can provide excellent performance with good stability robustness for systems with periodic disturbances. As will be shown, the system is phase stable at the disturbance frequency and gain stable everywhere else. High levels of disturbance attenuation can be obtained. For simple cases, (SISO, linear, open-loop stable, and a constant disturbance frequency) the compensator design parameters consist of the plant gain and phase at the disturbance frequency. The resulting low-order filter is easy to implement.

NARROWBAND CONTROL ATTRIBUTES
(open-loop stable)

Stability robustness

- **phase stable at disturbance frequency**
- **gain stable everywhere else**

Excellent performance

- **high levels of attenuation**

Simple design and implementation

- **model consists of plant gain and phase at disturbance frequency**
- **low order filter for coding**

Numerous approaches exist to the narrowband disturbance control problem, including classical feedback and adaptive feedforward. An excellent survey of the different types of narrowband control approaches is found in (ref. 2). The performance of these algorithms, however, can be made similar, at least for the relatively simple problem of controlling a SISO, linear, open-loop stable plant that has a constant disturbance frequency. The implementation of these control algorithms, however, can differ significantly.

NARROWBAND CONTROL APPROACHES

Feedback

- **classical control, bandpass filtering**
- **modern control, frequency-shaped cost functionals**
- **disturbance accommodating control**

Feedforward

- **knob turning**
- **adaptive feedforward filtering**
- **higher harmonic control**

Others

- **good survey in Sievers, L.A., vonFLotow, A.H., "Comparison and Extensions of Control Methods for Narrowband Disturbance Rejection". NCA-Vol.8, A.S.M.E. Winter Annual Meeting, Dallas, Texas, November 1990**

In the classical feedback approach, shown in the block diagram below, the compensator gain H(s) is made infinite at the disturbance frequency ω_d and small elsewhere. Typically this is implemented with a second-order filter, an undamped oscillator. The transfer function is shown below, where k is the compensator gain and ω_d is the disturbance frequency. Because the feedback gain is infinite, the net error will be driven to zero, if the system is stable.

The stability of this narrow-band controller is easily analyzed with the use of a Bode plot of loop gain. On the following page is a loop transfer function that assumes a constant gain plant (G(s) = g). This plot can be roughly divided into two frequency ranges, frequencies near the disturbance frequency and frequencies not near the disturbance frequency. At the disturbance frequency, the loop gain becomes infinite and changes phase by 180 degrees, because of the undamped oscillator poles in the compensator. At frequencies not close to the disturbance frequency, the loop gain is small, well below 0 db. As a result of these small gains elsewhere, the system stability is determined only by the loop gain near the disturbance frequency. The loop phase changes from +90 degrees to -90 degrees at the disturbance frequency because of the zero in the compensator transfer function. Thus the phase margin, which is the amount the plant phase can change before the system becomes unstable, is seen to be ± 90 degrees. The gain margin, which is the amount the plant gain can change before the system becomes unstable, is theoretically infinite.

CLASSICAL FEEDBACK APPROACH

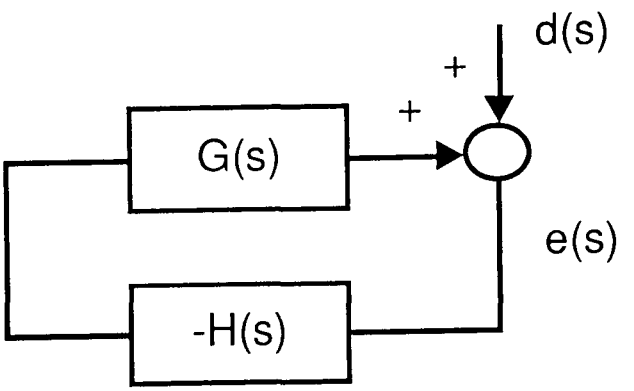

Best performance

$$H(s) = k \frac{s}{\left(\frac{s}{\omega_d}\right)^2 + 1} = \frac{H_{num}(s)}{\left(\frac{s}{\omega_d}\right)^2 + 1}$$

Best stability

$$\angle G(j\omega_d) + \angle H_{num}(j\omega_d) = +90°$$

These good stability margins were derived for a particularly simple plant that has constant gain. However, many of these good stability properties remain even under significantly relaxed assumptions about the plant. For a more general plant all we need know to design the compensator and analyze its stability properties is the maximum gain of the plant G_{max} and the phase of the plant at the disturbance frequency $\angle G(j\omega_d)$. At frequencies away from the disturbance frequency, we can guarantee stability if the loop gain is kept below 0 db independent of the plant phase, that is we "gain stabilize" the plant at these frequencies. If the loop gain is less than one (0 db) it can never encircle the minus one point on the Nyquist plot, which is the stability condition for this system. At frequencies near the disturbance frequency, the loop gain becomes infinite and the best stability robustness will be achieved if the loop gain changes from +90 to -90 degrees. The undamped poles in the compensator will contribute a change in loop phase of -180 degrees to the loop gain at the disturbance frequency. Therefore at the disturbance frequency we want the plant phase and the numerator portion of the compensator to contribute +90 degrees of phase. This stability definition was shown on the previous page (ref. 3). The numerator of the compensator, is therefore designed to satisfy this equation, once the plant angle at the disturbance frequency is known. The angle of the compensator can be changed by changing the zero structure or, with a discrete time implementation, by the use of a pure time delay. The gain of the compensator is chosen so that the maximum loop gain in frequency ranges not close to the disturbance frequency gives a desired gain margin.

LOOP TRANSFER FUNCTION

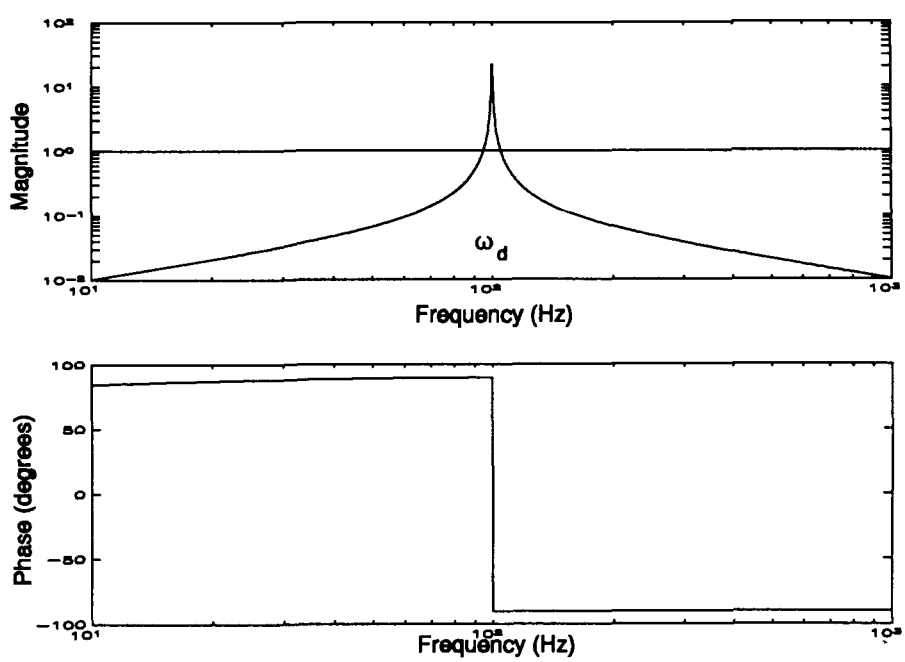

More explicitly, the closed-loop performance of the compensator is given by the sensitivity transfer function below. If we assume for simplicity that the plant transfer function G(s) is a simple unity gain, the closed-loop transfer function between the periodic disturbance d(s) and the net output error e(s) is given in the figure below. As expected, the error will be zero at the disturbance frequency, because of the infinite gain in the feedback compensator at this frequency. Note that although the shape of the closed-loop disturbance to error transfer function of the figure below is in general a function of the plant gain G(s), it will always be zero at the disturbance frequency ω_d independent of the plant gain at this frequency $G(j\omega_d)$. This is assuming that the plant is reasonably well behaved at the disturbance frequency, in particular that it does not have undamped zeros at the disturbance frequency. The relatively simple compensator, therefore, exhibits "perfect" performance in rejecting the disturbance force, if it is stable.

CLOSED LOOP TRANSFER FUNCTION

$$\frac{e(s)}{d(s)} = \frac{1}{1 + G(s)H(s)}$$

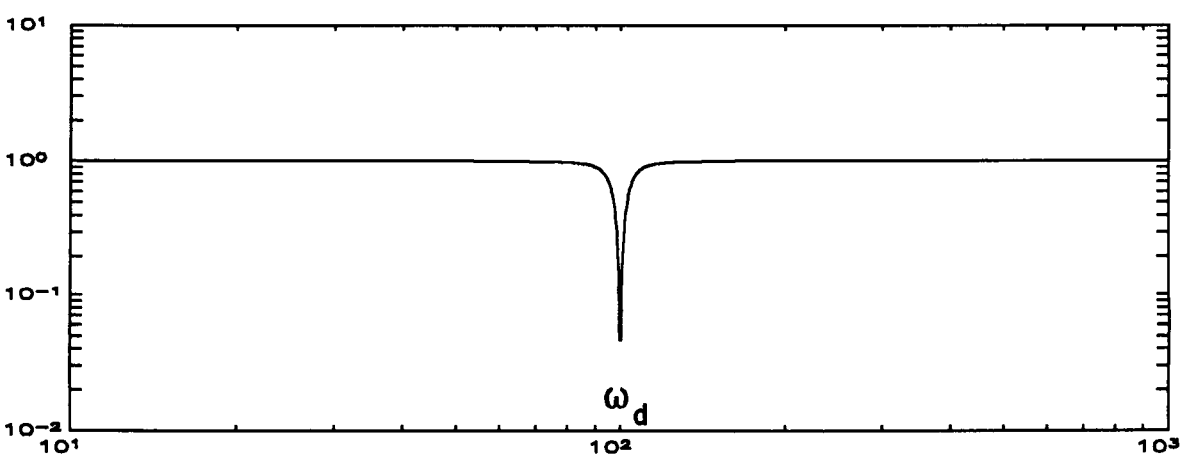

One application of this classical feedback narrowband control theory is to actively control a Stirling-cycle cryocooler compressor to cancel the higher harmonic forces produced by the linear motor (ref. 3). The linear motor is driven at a fundamental frequency of 40 Hz and produces higher harmonics that exceed the desired force vibration levels, as shown by the dotted plot in the figure below. The narrowband feedback compensation consists of five undamped oscillators, in parallel, at the higher harmonics of 80, 120, 160, 180, and 220 Hz. As shown in the figure, the forces at the target higher harmonics were driven into the noise floor of the force dynamometer, with over 40 db reduction at the 80 Hz harmonic.

AXIAL VIBRATION FORCE SPECTRA USING SELF-CANCELING CONFIGURATION: FIVE HARMONICS CANCELED

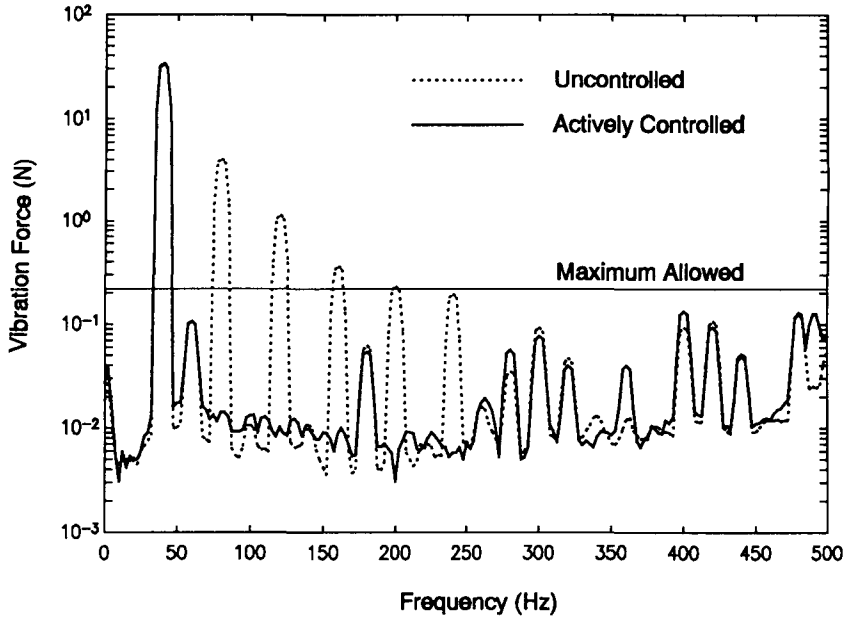

The previous discussion on narrowband control theory was assuming an open-loop stable plant. Attractive force magnetic bearings, however, are open-loop unstable. As a result, the loop transfer function cannot have small gains everywhere besides the disturbance frequency, as in the open-loop case, and still remain stable. There are numerous narrowband control approaches for synchronous vibration reduction of magnetic bearing systems, several of those are listed below (ref. 4,5,6). The remaining discussion will describe a SatCon hardware demonstration and introduce disturbance accommodating control theory as an effective narrowband approach for open-loop unstable plants.

NARROWBAND CONTROL FOR MAGNETIC BEARING SYSTEMS

- **magnetic bearing systems are open-loop unstable plants**
- **gain margin approach breaks down for open-loop stable plants breaks down**

Approaches

- **Notch filter**
- **Open-loop dynamic balancing**
- **LQ frequency shaping**
- **Disturbance accommodating control**
- **Others**

The following discussion applies specifically to a hardware demonstration developed by SatCon Technology Corporation (ref 7). The system, shown in the figure below, is a one-fifth scaled model (by mass) of a cryogenic alternator. The figure is an axial cross-section of the shaft and several important components, namely the magnetic thrust and journal bearings, the motor and the flywheels. The magnetically suspended rotor/shaft assembly mass is approximately 82 kilograms. The axis of rotation is in the vertical direction, therefore its weight is supported entirely by the thrust bearings. The induction motor spins the entire rotor/shaft assembly at a maximum working rotational speed of 3600 rpm (60 Hz). The flywheel components are simply cylindrical masses that simulate the inertial effects of the exciter and generator on the full scale cryogenic alternator. During cryogenic operation, the lower radial and axial actuators and the corresponding sensors are immersed in liquid nitrogen to demonstrate working bearings at 77°K.

CROSS-SECTION OF ROTOR/SHAFT ASSEMBLY

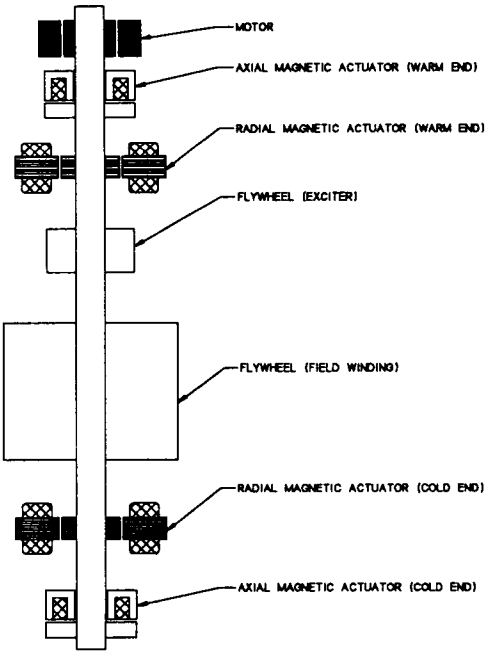

mass = 82 kg
shaft length = 1.2 m (47 in)
rotational speed = 3600 rpm (60 Hz, 377 rad/sec)
thrust bearing force (max) ≈ 800 N per bearing
radial bearing force (max) ≈ 400 N per bearing

The figure below is a photograph of the actual shaft, again showing the important components. The rotor is equipped with a adjustable mass system. The mass imbalance distance is increased by dropping a small weight down an access hole in the center of the shaft. When the shaft spins, the weight moves up a plugged-end channel, which is cut into the large flywheel, and thereby increases the mass imbalance.

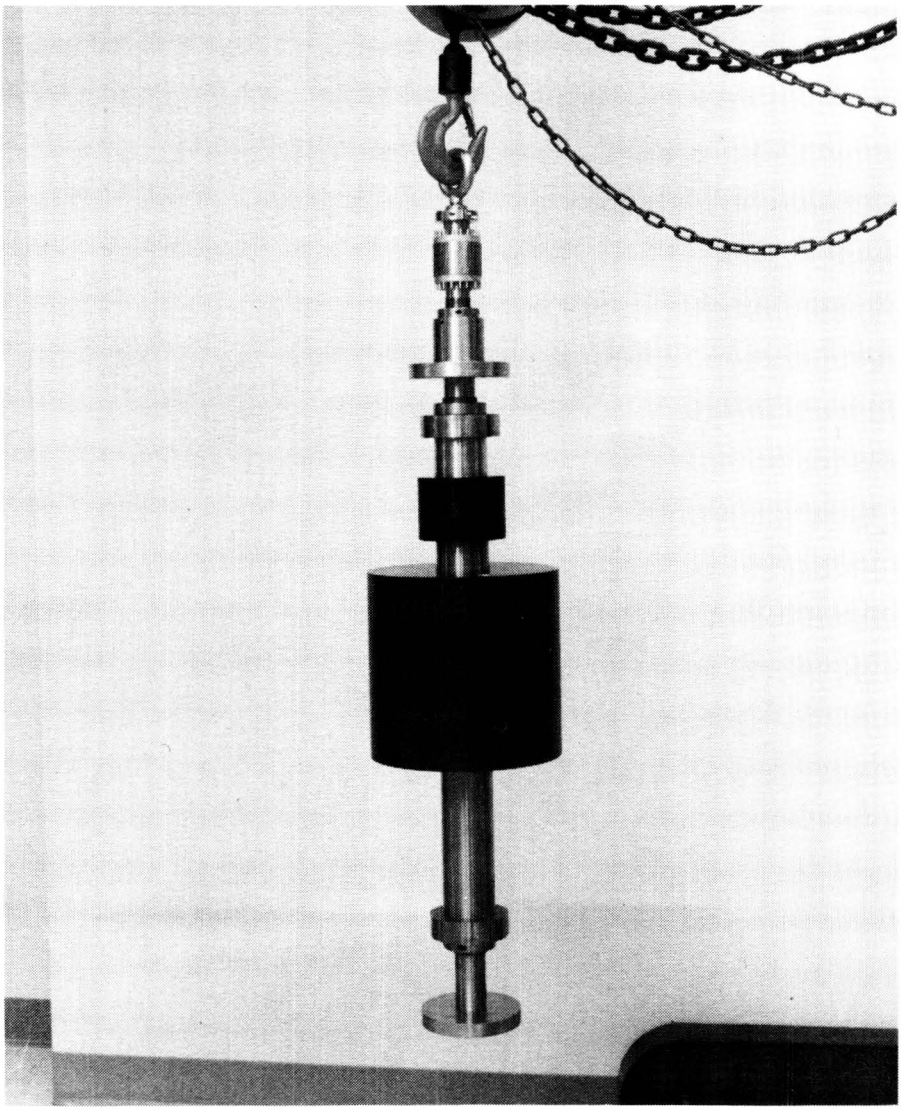

ORIGINAL PAGE
BLACK AND WHITE PHOTOGRAPH

A photo of the testbed structure is presented in the figure below. The shaft is vertical to accommodate for the cryogenic demonstration. As shown, a support stand provides the principal support and positioning of the entire system. A thick steel plate is bolted to the top of the stand. From this plate are hung the magnetic actuators, the rotating assembly, and the cryostat. During cryogenic operation, a level sensing system feeds liquid nitrogen to the cryostat from an external storage bottle. As a result, the bottom radial and axial magnetic actuators are submerged in liquid nitrogen and reach a constant temperature of 77°K. The magnetic actuator assembly consists of upper and lower housing structures which hold and accurately position the axial and radial actuators by the spacer also shown in the figure. Touch-down surfaces are also integrated into these housings in the event of interruption of power to the actuators. Various sensor systems including capacitive sensors for measuring radial and axial distances and accelerometers for measuring relative housing vibration are integrated into each housing.

Disturbance accommodating control (DAC) theory is used to design controllers and estimators for systems with disturbances having waveform structure (ref. 8). The control of magnetic bearings is a natural application of DAC theory because the dominant disturbances are non-stochastic functions of the synchronous frequency, as previously described. DAC theory is used in the following discussion to develop a disturbance model of the measurement error. By combining the plant and disturbance models, an accurate estimate of the true center of mass position is created. Then the corresponding controller feeds back an uncorrupted estimate of the center of mass position, which results in the desired behavior of spinning about the center of mass.

DISTURBANCE ACCOMMODATING CONTROL (DAC)

Applications

- o disturbances have "waveform" structure
- o non-stochastic methodology

Approach

- o develop disturbance model
- o combine plant and disturbance models to design estimator
- o given this structure, use appropriate tools to design controller

Attributes

- o good in rotor dynamic problems
- o does not affect stability
- o quick convergence of estimates

A block diagram of the closed loop DAC system is presented in the figure below. The system consists of the actual plant, the plant and disturbance models and the controller. The plant and disturbance models make up the DAC estimator. The disturbance model represents the measurement error disturbance at each sensor. The disturbance estimates are injected at the plant model output, thereby producing estimates of the corrupted measurements. The differences in the estimated and actual measurements are fed back through the estimator gains to drive the plant and disturbances estimation errors to zero. The purpose of the disturbance model is to be able to distinguish between the plant and disturbance states, in the presence of disturbances. By feeding back the estimated inertial positions, uncorrupted by the synchronous disturbances, the rotor will spin about its inertial axis. For a variable speed system, the rotational speed is fed to the controller to update the disturbance model. Hence, the oscillator will track the rotational speed and reduce the vibrations as the speed changes.

BLOCK DIAGRAM OF DAC SYSTEM

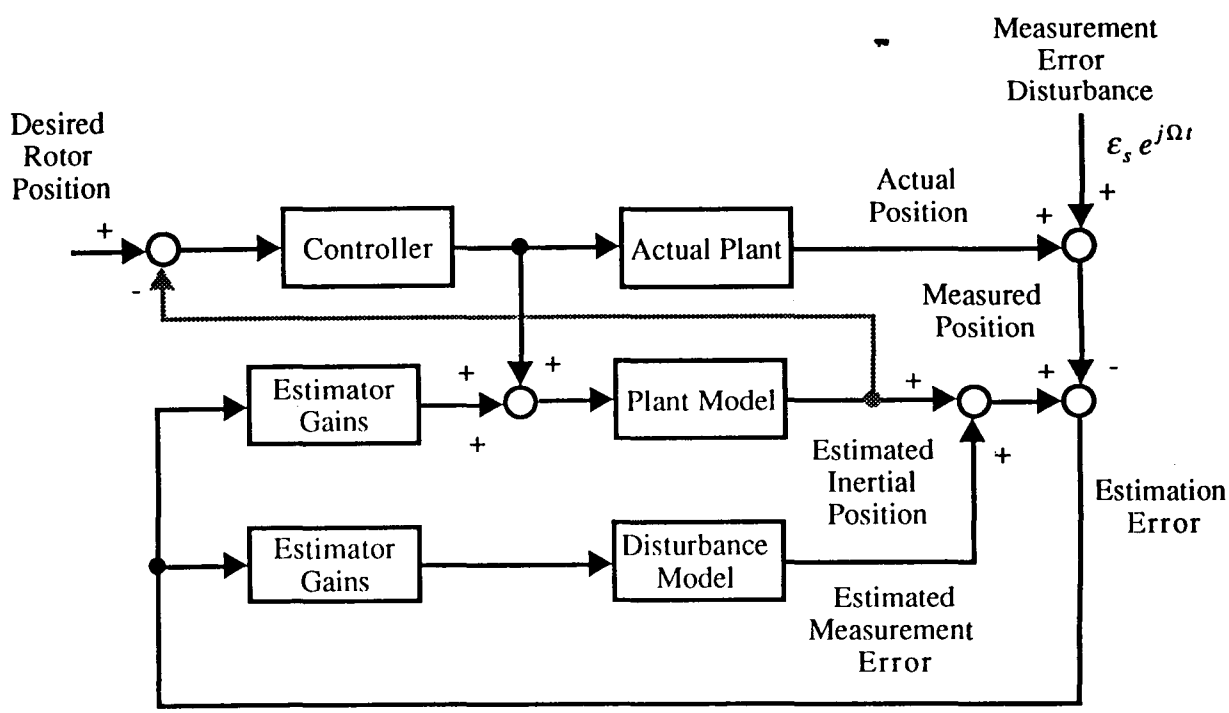

The figure below is a plot of the singular values of the closed loop transfer function matrix from the measurement error disturbance inputs to the inertial position outputs. The area of interest is at 60 Hz, the rotational frequency. The infinite notch at 60 Hz illustrates that the measurement error disturbance is completely removed from the system. It is important to note that both the maximum and the minimum singular values are zero at 60 Hz, resulting in complete ideal attenuation of the measurement error disturbances.

SINGULAR VALUE PLOT
FROM MEASUREMENT ERROR DISTURBANCE TO INERTIAL POSITION

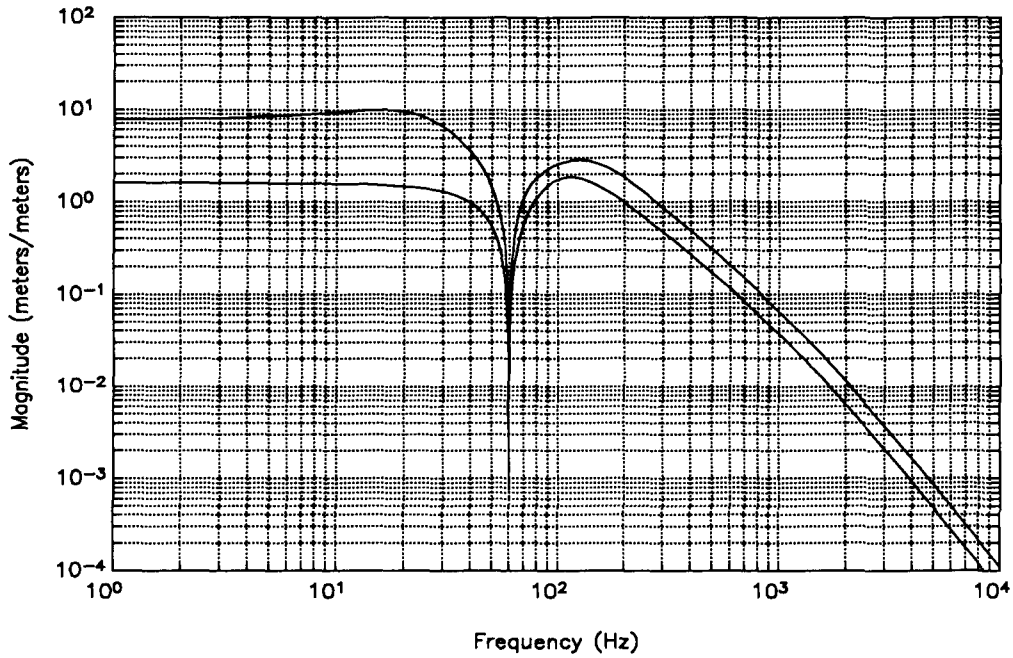

The notch does not occur in the transfer function between the commanded input and the inertial output as shown in the figure below. The DAC estimator, unlike a notch filter, rejects the synchronous disturbances without attenuating the control signals at 60 Hz. The system is therefore stable at all rotational speeds.

SINGULAR VALUE PLOT
FROM COMMANDED INPUT TO INERTIAL POSITION

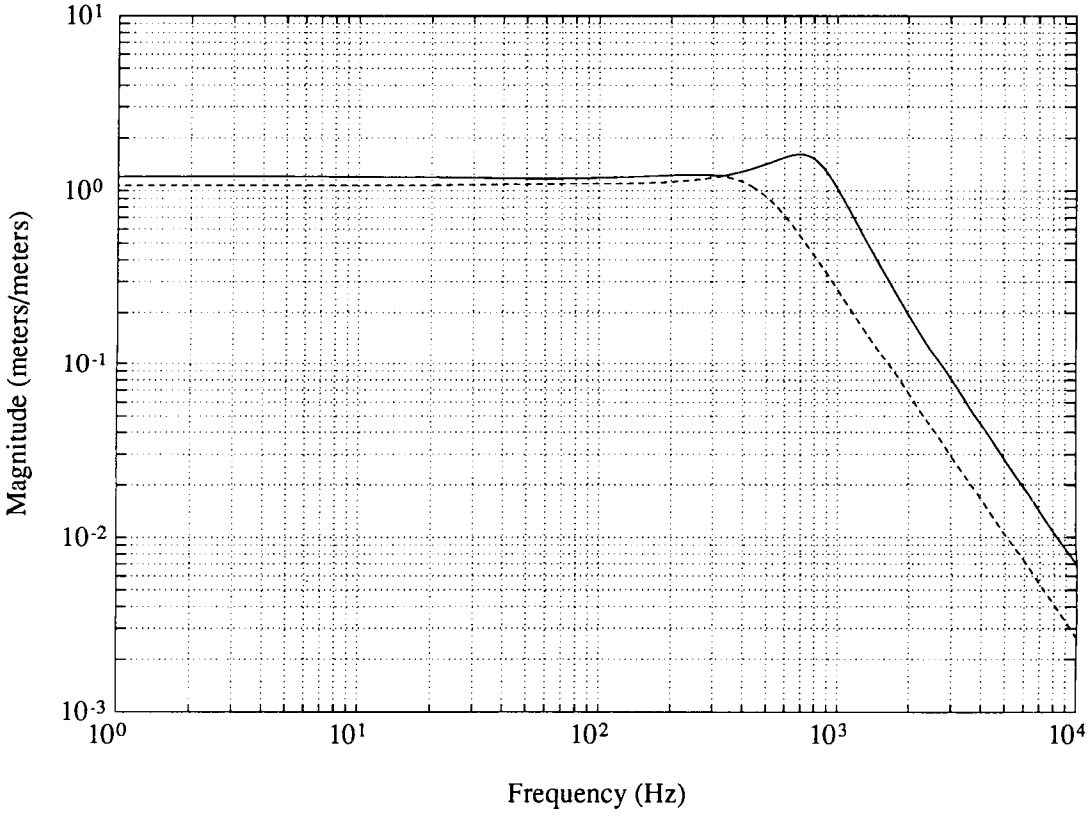

The figure presented below is the time simulation of the inertial position response to the measurement error disturbance input. At negative time, the rotor is spinning around its geometric center because the feedback variables are the measured positions. Then at time t=0, the DAC estimator is turned on and the feedback variable becomes the estimated center of mass position. As a result of the DAC estimator, the rotor quickly reaches the desired steady-state position, spinning about its inertial axis. This graph represents the motion of the inertial positions in the X plane. Due to symmetry, the Y plane is identical, 90 degrees out of phase.

CENTER OF MASS POSITION RESPONSE TO MEASUREMENT ERROR DISTURBANCE

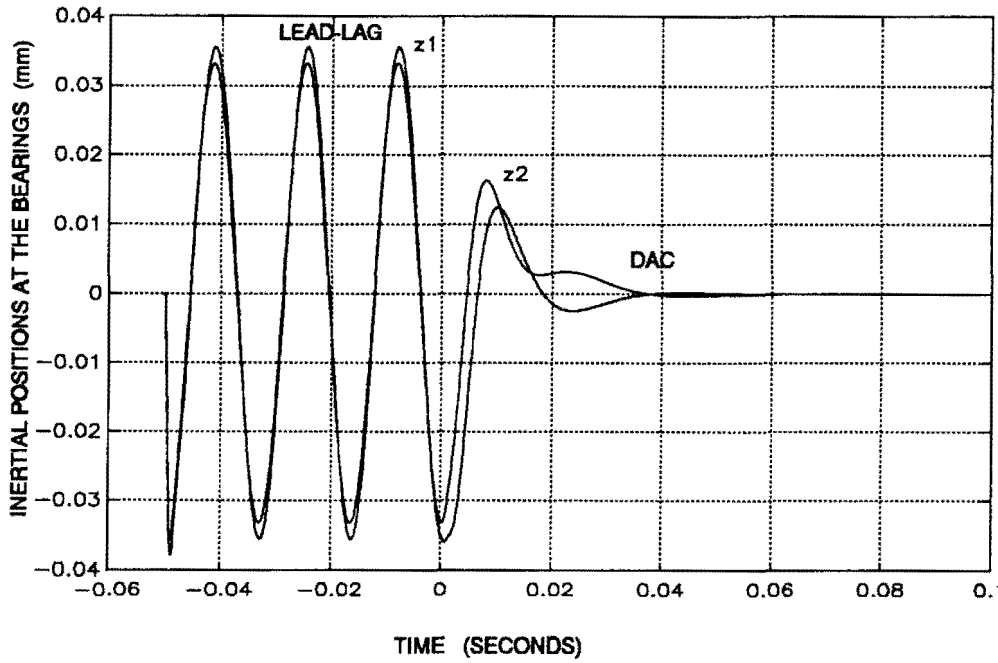

The bearing force response to the measurement error disturbance is shown in the figure below, again illustrating the dynamics of the X plane. The DAC estimator is turned on at time t=0, hence the feedback variables are changed from the corrupted measurement positions to the estimated inertial positions. As shown, the forces on the rotor are reduced significantly.

CENTER OF MASS FORCE RESPONSE TO MEASUREMENT ERROR DISTURBANCE

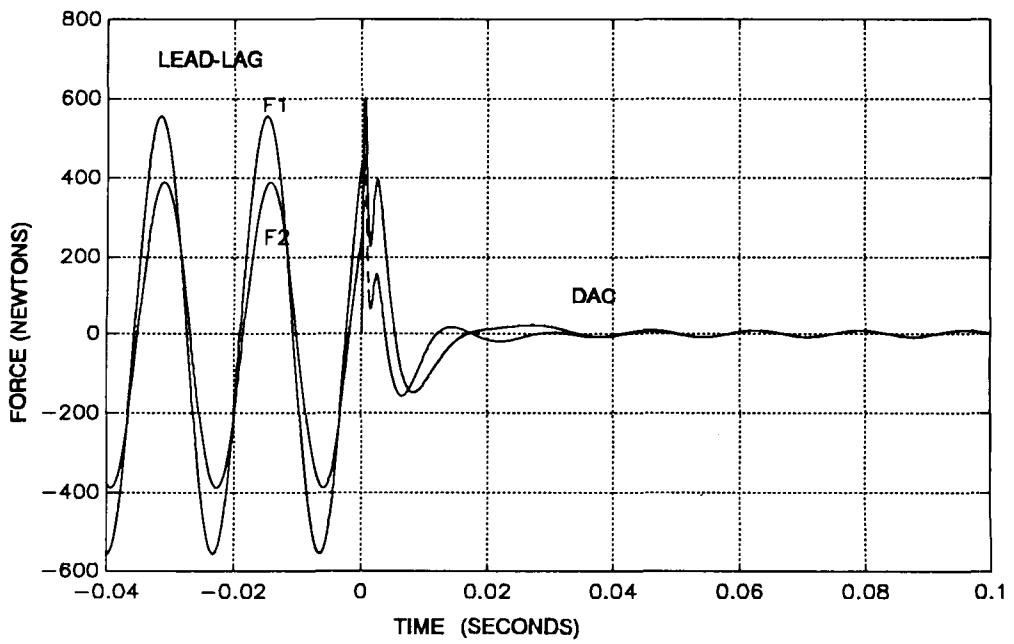

References

1. Gaffney, M.S. "Synchronous Vibration Reduction In Magnetic Bearing Systems". S.M. Thesis, Massachusetts Institute of Technology, Cambridge, Massachusetts, June 1990.

2. Sievers, L.A., vonFlotow, A.H., "Comparison and Extensions of Control Methods for Narrowband Disturbance Rejection". NCA-Vol.8, A.S.M.E. Winter Annual Meeting, Dallas, Texas, November 1990

3. Johnson, B.G., Gaffney, M.S. "Demonstration of Active Vibration Control on the JPL Cryocooler Vibration Testbed". SatCon Technology Corporation Final Report R30-91, Cambridge, MA, August 1991

4. Johnson, B.G, Hochney, R.L., Misovec, K.M. "Active Synchronous Response Control of Rigid-Body Rotors". IMechE 4th International Conference on Vibrations Machinery, September, 1988

5. Humphris, R.R., Knospe, C.R., Sundaram, S. "Dynamic Balancing With Open Loop Control of Magnetic Bearings". 26th Annual IECEC, Boston, MA, August 1991

6. Gaffney, M.S., Johnson, B.G., "Application of Disturbance Accommodation Control to Reduce Vibrations in Magnetic Bearing Systems". NCA-Vol.8, A.S.M.E. Winter Annual Meeting, Dallas, Texas, November 1990

7. Downer, J.R., et. al., "Cryogenically-Cooled Magnetic Journal Bearings". SatCon Final Report R08-91, Cambridge, MA, March 1991

8. Johnson, C.D., "Theory of Disturbance Accommodating Controllers, Chapter 7, Control and Dynamic Systems Vol. 12 (D.T. Leondes, Ed.), Academic Press, New York, 1976